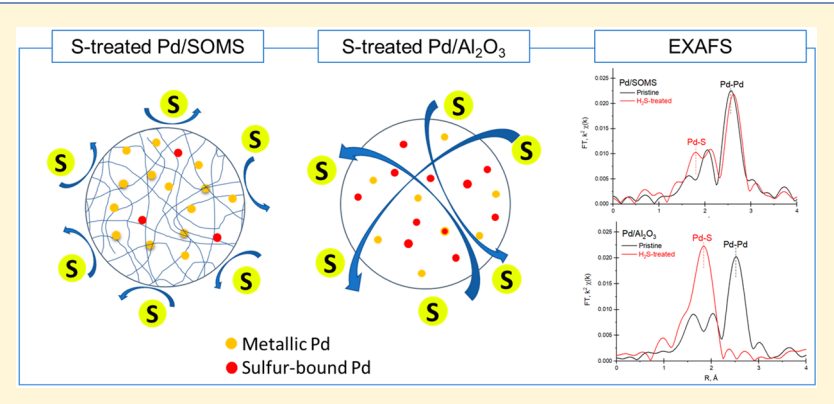


# Aqueous-Phase Hydrodechlorination of Trichloroethylene over Pd-Based Swellable Organically Modified Silica: Catalyst Deactivation **Due to Sulfur Species**

Gokhan Celik,<sup>†</sup> Saurabh A. Ailawar,<sup>†</sup> Seval Gunduz,<sup>†</sup> Jeffrey T. Miller,<sup>‡</sup> Paul L. Edmiston,<sup>§</sup> and Umit S. Ozkan\*,†

Supporting Information



ABSTRACT: One of the problems of catalytic water treatment systems is that sulfur-containing species present in contaminated water have a detrimental effect on the catalytic performance because of strong interactions of sulfur species with active metal sites. In order to address these problems, our research has focused on developing a poison-resistant catalytic system by using a novel material, namely, swellable organically modified silica (SOMS), as a catalyst scaffold. Our previous investigations demonstrated that the developed system was resistant to chloride poisoning, active metal leaching, and carbon deposition under reaction conditions. This study examines the sulfur tolerance of the developed catalytic system for hydrodechlorination (HDC) of trichloroethylene (TCE) by subjecting Pd-incorporated samples to different sulfur species, including sulfates (SO<sub>4</sub><sup>2-</sup>), bisulfides (HS<sup>-</sup>), and hydrogen sulfide (H<sub>2</sub>S). The pristine and sulfur-treated catalysts were then tested for aqueous- and gas-phase HDC of TCE and characterized by several techniques, including N2 physisorption, X-ray photoelectron spectroscopy (XPS), extended X-ray absorption fine structure spectroscopy (EXAFS), and temperatureprogrammed reaction  $(TP_{rxn})$  with  $H_2$ . The investigations were also performed on  $Pd/Al_2O_3$ , a commercially used HDC catalyst, to have a basis for comparison. The activity and characterization results revealed that Pd/Al<sub>2</sub>O<sub>3</sub> underwent deactivation due to exposure to sulfur-containing compounds. Pd/SOMS, however, exhibited better resistance to aqueous sulfates, bisulfides, and gas-phase H<sub>2</sub>S. In addition, the removal of sulfur species from completely poisoned catalysts was found to be more facile in Pd/SOMS than Pd/Al<sub>2</sub>O<sub>3</sub>. The tolerance of Pd/SOMS to sulfur poisoning was attributed to stem from the novel characteristics of SOMS, such as swelling ability and extreme hydrophobicity.

# 1. INTRODUCTION

Supported metal catalysts are sensitive to sulfur and readily deactivate on the basis of the duration of the exposure, the concentration, and the chemical form of the sulfur species. 1-4 For this reason, developing deactivation-resistant catalytic systems has been one of the important topics of catalysis research in general. On the basis of literature on the hydrodechlorination (HDC) of trichloroethylene (TCE), the state-of-the-art HDC catalysts do not perform well in real

groundwater because of the sulfur-containing species that strongly adsorb on the catalytically active sites. 1,5-9 It has been reported that even ppm levels of the sulfur species are enough to deactivate the HDC catalysts. 1,6,10 These sulfur species can

Received: December 3, 2018 Revised: February 7, 2019 Accepted: February 14, 2019 Published: February 14, 2019

William G. Lowrie Department of Chemical and Biomolecular Engineering, The Ohio State University, 151 W. Woodruff Avenue, Columbus, Ohio 43210, United States

<sup>&</sup>lt;sup>‡</sup>Davidson School of Chemical Engineering, Purdue University, 480 Stadium Mall Drive, West Lafayette, Indiana 47907-2100, United States

<sup>§</sup>Department of Chemistry, The College of Wooster, 943 College Mall, Wooster, Ohio 44691, United States

be in different chemical forms, such as  $\mathrm{SO_4}^{2-}$ ,  $\mathrm{SO_3}^{2-}$ ,  $\mathrm{HS}^-$ , or  $\mathrm{S^{2-}}$ , at varied concentrations. <sup>1,5,6</sup> They originate from improper sulfur-containing discharges and dissolution of sulfate-containing minerals in groundwater. <sup>11</sup> Although sulfate molecules are less deleterious than reduced sulfur species, such as bisulfides and sulfites, the conversion of sulfates to reduced sulfur species is thermodynamically favorable under HDC reaction conditions. <sup>6,12,13</sup> In addition, the transformation of sulfates to sulfur species naturally occurs in groundwater by anaerobic bacterial activities. <sup>1,12</sup>

The deactivation effects due to sulfur compounds can be minimized by altering the operating parameters of HDC systems. One approach is to adjust the pH of groundwater. 1,8 Angeles-Wedler et al. studied the deactivation characteristics of Pd/Al<sub>2</sub>O<sub>3</sub> at different pH values of the reaction solution. They found that the degree of deactivation was higher for acidic groundwater, indicating that the pH of the water is an essential parameter to mitigate the deactivation effects due to sulfur compounds. At high pH values, the Pd-S interaction can be suppressed.<sup>6,8</sup> Munakata and Reinhard obtained a rate expression that takes the acidity of water and the concentration and types of sulfur species into account in describing the catalyst deactivation. Another approach is to oxidize the reduced sulfur compounds to sulfates that do not have a high affinity for Pd sites. 6,8,12,13 In 2008, Angeles-Wedler et al. added permanganate to the feed stream of a HDC reactor to protect the Pd sites by oxidizing the reduced sulfur species before they enter the reactor and poison the catalyst. Although addition of permanganate was successful in oxidizing the reduced sulfur species and ceasing the microbial activity, inhibition of Pd and oxidation of TCE were observed at high concentrations of permanganate.8,12

The deactivation effects due to sulfur compounds can also be minimized by developing poison-resistant catalytic materials. Wong and co-workers designed a highly active and stable bimetallic catalyst with a Pd-shell/Au-core structure. 14,15 The Pd-Au nanoparticles exhibited improved resistance to sulfides due to the electronic effects of Au on Pd and the formation of Pd-Au catalytic sites. 16 Hydrophobic materials were also used to circumvent the deactivation issues. Schüth et al. developed a Pd-based catalytic system by altering the pore size and hydrophobicity of zeolite-Y, which exhibited better poisonresistance than other studied catalysts, including Pd-containing alumina, MCM-41, and ZSM-5. 17,18 Kopinke and co-workers reported that Pd-based hydrophobic materials are more resistant to sulfur poisoning. 9,12 However, polydimethylsiloxane, which was used to coat Pd/Al<sub>2</sub>O<sub>3</sub> to increase its hydrophobicity, was degraded by the unavoidable reaction product HCl due to silicone hydrolysis. The resultant catalyst became more susceptible to sulfur poisoning. 9,19,20

We have previously demonstrated the use of a swellable organically modified silica (SOMS) to mitigate the deactivation problems of Pd-based HDC catalytic systems. <sup>21–25</sup> SOMS is a novel catalyst scaffold that has unique properties, such as high affinity for adsorbing organic compounds, extreme hydrophobicity, swelling ability upon contact with organics, and high surface area. <sup>21–29</sup> By using SOMS as a scaffold, an animated Pd-based catalyst, the characteristics of which change upon exposure to organic compounds, was synthesized. These unique characteristics led us design poison-resistant catalysts by incorporating Pd NPs inside the matrix of a SOMS scaffold. <sup>21,24</sup> Pd/SOMS showed remarkable resistance to chloride poisoning and Pd leaching by HCl. <sup>23,24</sup> In addition,

due to its surface hydroxyl groups and low acidity, Pd/SOMS was also shown to be resistant to coke deposition during gasphase HDC of TCE. In this contribution, Pd/SOMS was studied further to evaluate its resistance to sulfur-containing species. Pd/SOMS was exposed to different sulfur species, including SO<sub>4</sub><sup>2-</sup>, HS<sup>-</sup>, and H<sub>2</sub>S. Investigations were also performed over the commonly used HDC catalyst Pd/Al<sub>2</sub>O<sub>3</sub> in order to have a basis for comparison.

# 2. EXPERIMENTAL SECTION

**2.1. Catalyst Synthesis.** The synthesis procedure of SOMS was previously described by Edmiston and coworkers. Pd incorporation to SOMS was performed by incipient wetness impregnation with a target metal loading of 1 wt %. The required amount of Pd(II) acetate (Sigma-Aldrich 99.9%) was dissolved in acetone and then added to the SOMS support dropwise using a micropipet until the support was saturated with the solution. The saturated SOMS was dried at room temperature. The saturation—drying cycle was repeated until the precursor solution was depleted. The reduction of Pd nanoparticles was performed by NaBH<sub>4</sub> dissolved in 95% ethanol. The reduced catalyst was filtered, washed with ethanol several times, and dried in an oven at 70 °C overnight.

 $Pd/Al_2O_3$  (1 wt %) was purchased from Sigma-Aldrich and reduced at 350 °C under H<sub>2</sub>.

- **2.2. Exposure to Aqueous-phase Sulfur Species.** The pristine Pd/SOMS and Pd/Al $_2$ O $_3$  samples were treated in the aqueous solutions of Na $_2$ SO $_4$  and NaHS at varied concentrations at room temperature. These experiments were conducted in a 500 mL three-neck flask in an inert environment. The catalyst powders and the solution containing sulfur species were subsequently introduced into the flask. The poisoning treatment was performed for 1 h under vigorous stirring. The solution was then filtered and the resultant poisoned catalyst was dried. In the treatments where Pd/SOMS was swollen, ethanol was used as an organic swelling agent at different concentrations.
- **2.3. Nitrogen Physisorption.** The textural properties of the pristine and poisoned samples of Pd/Al<sub>2</sub>O<sub>3</sub> and Pd/SOMS catalysts were examined by conducting N<sub>2</sub> physisorption experiments on an accelerated surface area analyzer and porosimetry instrument (Micromeritics ASAP 2020) at 77K. Before the analysis, samples were degassed at 120 °C and 2  $\mu$ mHg. The Brunauer–Emmett–Teller (BET) isotherm was used to determine the surface area. The Barrett–Joiner–Halenda (BJH) method was used to determine the pore size, pore volume, and pore size distribution.
- **2.4.** X-ray Photoelectron Spectroscopy (XPS). The nature of sulfur species accumulated on poisoned Pd/Al<sub>2</sub>O<sub>3</sub> and Pd/SOMS catalysts was investigated by XPS. The experiments were carried out in a Kratos Ultra Axis spectrometer equipped with a monochromatized Al K $\alpha$  X-ray source operating at 12 kV and 10 mA. The samples were loaded on a carbon tape and placed in the chamber. After evacuation overnight, a survey scan, followed by high-resolution region scans, was acquired. The charging effects were corrected with respect to C 1s (284.5 eV). CasaXPS 2.3.16 software was used to perform deconvolution and data analysis.
- **2.5. Extended X-ray Absorption Fine Structure (EXAFS).** The nature of Pd NPs and the changes in the atomic environment of Pd due to poisoning by sulfur species

were investigated by EXAFS spectroscopy. Experiments were performed at Pd K-edge (24 350 eV) in transmission mode with quick scans on the insertion device beamline of the Materials Research Collaborative Access Team (MRCAT-10ID) at Advanced Photon Source at Argonne National Laboratory. A cryogenically cooled double-crystal Si(111) monochromator was used with a Pt-coated mirror to minimize the presence of harmonics. Samples in powder form were loaded into a cylindrical sample holder having six wells. Energy alignment was performed with respect to a simultaneously collected spectrum of a Pd foil. The Pd edge energy was determined as the position of the maximum of the first peak in the first derivative of the XANES region. Standard procedures outlined by Ressler were followed to extract EXAFS data by using WINXAS 3.2. software.<sup>30</sup> Pd foil, Pd oxide, and Pd chloride trace-metal chemicals were used as reference materials to obtain phase shifts and backscattering amplitudes for Pd-Pd (12 at 2.75 Å), Pd-O (4 at 2.05 Å), and Pd-S (4 at 2.31 Å), respectively.

2.6. Gas-Phase H<sub>2</sub>S Treatment. Pd/SOMS and Pd/Al<sub>2</sub>O<sub>3</sub> catalysts were exposed to gas-phase H2S in a plug flow reactor at 250 °C. The poisoning procedure was adapted from Pazmino et al.<sup>31</sup> The pristine sample was loaded into a reactor and placed inside a furnace, where the temperature was controlled. Following a flushing step at room temperature with He at a flow rate of 80 mL/min, the temperature was increased to 250 °C. After flowing He for 30 min, the catalyst samples were exposed to a H<sub>2</sub>S-containing gas stream (800 ppm of H<sub>2</sub>S, 25% H<sub>2</sub>, and balance He) for 3 h. This treatment was performed in the presence of 25% H<sub>2</sub> to prevent the agglomeration of Pd sulfide clusters. The effluent gas was sent to an AgNO3 bubbler and the precipitation of the AgS was verified. The H<sub>2</sub>S treatment was followed with H<sub>2</sub> flow for 1 h to remove reversibly adsorbed sulfur. Then, He was flowed through the reactor for 1 h and the temperature was decreased to room temperature.

**2.7. Temperature-programmed Reaction (TP**<sub>rxn</sub>) with  $H_2$ . Pd/SOMS and Pd/Al<sub>2</sub>O<sub>3</sub> samples treated with Na<sub>2</sub>SO<sub>4</sub> in the aqueous phase and  $H_2$ S in the gas phase were placed in a quartz reactor (ID = 4 mm, OD = O.25 in). The reactor then was placed into a Carbolite MTF 10/15/130 furnace. The outlet stream was connected to an online mass spectrometer (MKS-Cirrus II) operating in scanning ion mode to monitor the evolution of  $H_2$ S (m/z = 34) from the reactor. A 5%  $H_2$ / He gas stream was introduced to the reactor at a flow rate of 30 mL/min at room temperature. After obtaining a stable m/z = 34 signal, the temperature was increased at a ramp rate of 10 °C/min until 900 °C.

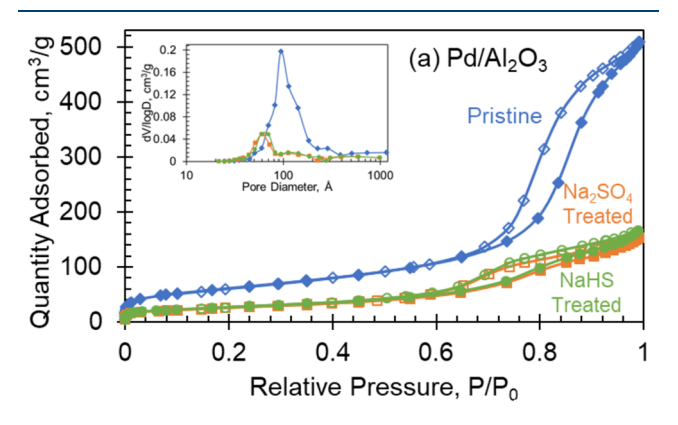
**2.8. Catalytic Activity Experiments.** 2.8.1. Aqueousphase Experiments. Pd/SOMS and Pd/Al<sub>2</sub>O<sub>3</sub> catalysts in their pristine and poisoned states were tested for aqueousphase HDC of TCE in a batch reactor operating at 50 bar and 30 °C. The operation of the reactor system was described in our previous publication. Briefly, a known amount of catalyst, in powder form, was loaded into a catalyst addition device (CAD), which was subsequently secured in the headspace of the reactor. The reactor, which contained 200 mL reaction solution, was flushed with He and the impeller was started. After stabilization of temperature and pressure, the CAD was activated to start the reaction. A sample was taken before the reaction started to determine the initial concentration of TCE, which was found to be approximately 250 ppm. The samples taken from the reactor throughout the reaction were

immediately analyzed using a high-performance liquid chromatograph (HPLC) equipped with a UV/vis detector (Shimadzu, SPD-20A) and a selective chloride electrode (Cole Palmer, UX-27504-08).

2.8.2. Gas-phase Experiments. The pristine and  $H_2S$ -treated Pd/SOMS and Pd/Al $_2O_3$  catalysts were tested in gas-phase HDC of TCE reaction using a bench-scale packed bed flow reactor system. The catalysts were packed in a quartz tube placed in a tubular furnace. The feed gas concentration was set to 0.7% TCE (TCE vapor was generated by using a glass bubbler that contained pure TCE), 21%  $H_2$ , and balance He. The reactor outlet was connected to an online gas chromatograph (Shimadzu Scientific 2010) equipped with a Q-bond column and a flame ionization detector (FID) for quantification of TCE conversion.

# 3. RESULTS AND DISCUSSION

**3.1.** Effect of Exposure to Aqueous Poisons. 3.1.1. Nitrogen Physisorption. The textural properties of Pd/Al<sub>2</sub>O<sub>3</sub> and Pd/SOMS catalysts before and after they were exposed to aqueous-phase sulfur compounds were examined by N<sub>2</sub> physisorption. Nitrogen adsorption—desorption isotherms and pore size distributions of pristine, Na<sub>2</sub>SO<sub>4</sub>-treated, and NaHS-treated samples of Pd/Al<sub>2</sub>O<sub>3</sub> are shown in Figure 1a. The pristine Pd/Al<sub>2</sub>O<sub>3</sub> exhibited a type-IV adsorption isotherm with H3-type hysteresis caused by capillary condensation of nitrogen.<sup>32</sup> Shown in the inset of Figure 1a, the pore size distribution of Pd/Al<sub>2</sub>O<sub>3</sub> centered around 10 nm. Upon poisoning Pd/Al<sub>2</sub>O<sub>3</sub> with sulfur-containing compounds,



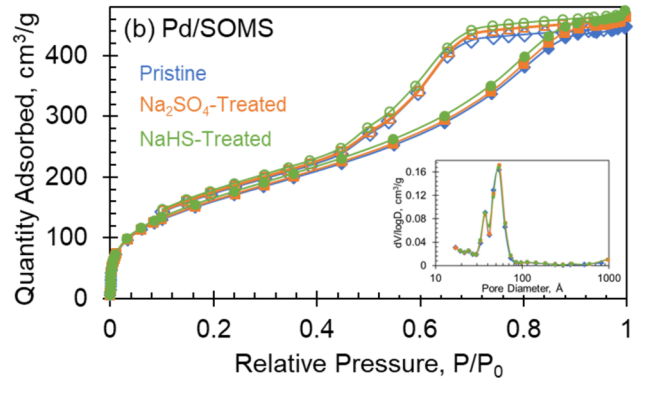


**Figure 1.** Nitrogen adsorption—desorption isotherms of pristine, 0.1 M Na $_2$ SO $_4$ -treated, and 0.1 M NaHS-treated (a) Pd/Al $_2$ O $_3$  and (b) Pd/SOMS. Insets: BJH pore size distributions of pristine, 0.1 M Na $_2$ SO $_4$ -treated, and 0.1 M NaHS-treated (a) Pd/Al $_2$ O $_3$  and (b) Pd/SOMS.

the type of the adsorption—desorption isotherm and hysteresis remained unchanged. The quantity of adsorbed nitrogen, however, decreased significantly. In addition, the pore size distribution of Pd/Al<sub>2</sub>O<sub>3</sub> poisoned by sulfur-containing compounds shifted to a lower pore diameter of around 6.5 nm, but this is likely due to a hydration effect, since a similar observation was made after the sample was soaked in water.

The adsorption—desorption isotherm of pristine Pd/SOMS (Figure 1b) exhibited monolayer adsorption at low relative pressures and type-IV adsorption isotherm. Two types of hysteresis were observed over pristine Pd/SOMS: (i) H2-type hysteresis caused by capillary condensation and (ii) swelling hysteresis observed at lower relative pressures. <sup>23,32,33</sup> The pore size distribution of Pd/SOMS centered at 5.4 and 3.7 nm. The 3.7 nm peak, however, was attributed to an artifact of nitrogen physisorption measurements. <sup>21,23,34</sup> Exposure to sulfur species did not result in any major changes in the adsorption—desorption isotherms, the type of hysteresis, and the pore size distribution. In addition, the swelling hysteresis was not affected by the sulfur treatments, suggesting that the swelling characteristic of Pd/SOMS was retained.

The  $N_2$  physisorption results of pristine, water-soaked,  $Na_2SO_4$ -treated, and NaHS-treated  $Pd/Al_2O_3$  are given in Table 1. The textural properties of pristine  $Pd/Al_2O_3$  were

Table 1. Textural Properties of Pristine, Na<sub>2</sub>SO<sub>4</sub>-Treated, and NaHS-Treated Pd/Al<sub>2</sub>O<sub>3</sub> and Pd/SOMS

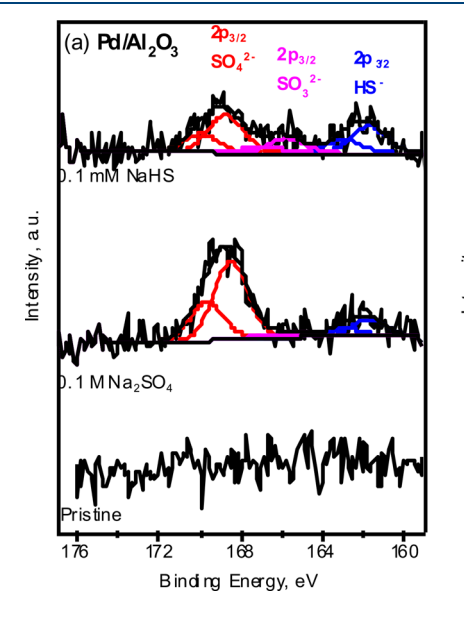
samples		BET surface area,m <sup>2</sup> /g	pore volume, cm <sup>3</sup> /g	pore diameter, nm
Pd/Al <sub>2</sub> O <sub>3</sub> pristine		220	0.79	10.3
	water-soaked	97	0.25	7.4
	$0.1 \text{ M Na}_2\text{SO}_4$	92	0.24	7.4
0.1 M NaHS		97	0.26	7.5
Pd/SOMS	pristine	590	0.73	3.9
	water-soaked	604	0.75	3.9
	$0.1 \text{ M Na}_2\text{SO}_4$	598	0.75	4.0
	0.1 M NaHS	612	0.74	4.2

adversely affected due to the treatments with aqueous solutions. The textural properties of water-soaked Pd/Al<sub>2</sub>O<sub>3</sub>, however, were not different from that of sulfur-exposed Pd/ Al<sub>2</sub>O<sub>3</sub>, indicating that the changes in the textural properties stemmed from soaking Pd/Al<sub>2</sub>O<sub>3</sub> in water, rather than interactions of Pd/Al<sub>2</sub>O<sub>3</sub> with sulfur-containing molecules. In our previous investigation, a similar behavior was observed when the catalysts were exposed to chloride-containing compounds. In that study, exposure to NaCl or HCl was shown not to have an additional adverse effect on the textural properties.<sup>23</sup> The changes in the textural properties were attributed to the surface hydration of Pd/Al<sub>2</sub>O<sub>3</sub>. It was reported that the formation of hydroxyl compounds easily occurs on the surface of Pd/Al<sub>2</sub>O<sub>3</sub> due to its hydrophilic nature. The complete removal of the surface hydration requires temperatures as high as 900 °C under atmospheric pressure.35,36

Table 1 also shows the textural properties of pristine, watersoaked, and sulfur-treated Pd/SOMS. The BET surface area, BJH pore volume, and BJH pore diameter of pristine Pd/SOMS were found to be 590  $\rm m^2/g$ , 0.73  $\rm cm^3/g$ , and 3.9 nm, respectively. Poisoning treatments did not affect the textural properties of Pd/SOMS. Considering that the changes in the textural properties of Pd/Al $_2$ O $_3$  stemmed from the surface hydration due to soaking in water, it is conceivable that the hydrophobic nature of Pd/SOMS suppressed the formation of surface hydration, resulting in no changes in textural properties.

3.1.2. X-ray Photoelectron Spectroscopy. X-ray photoelectron spectra of the S 2p region obtained over pristine samples of  $Pd/Al_2O_3$  and Pd/SOMS and those exposed to aqueous—phase sulfur compounds are shown in Figure 2. The spectra were deconvoluted by fitting S  $2p_{3/2}$  and  $2p_{1/2}$  peaks into a doublet with a spin—orbit splitting ratio of 2:1 and a fixed doublet separation of 1.18 eV.<sup>37</sup> The deconvolution results including binding energies (BE) and percentage composition of surface sulfur species are given in Table S1 of the Supporting Information.

As shown in Figure 2a, the S 2p spectrum of pristine Pd/Al<sub>2</sub>O<sub>3</sub> does not have any spectral features, indicating that the



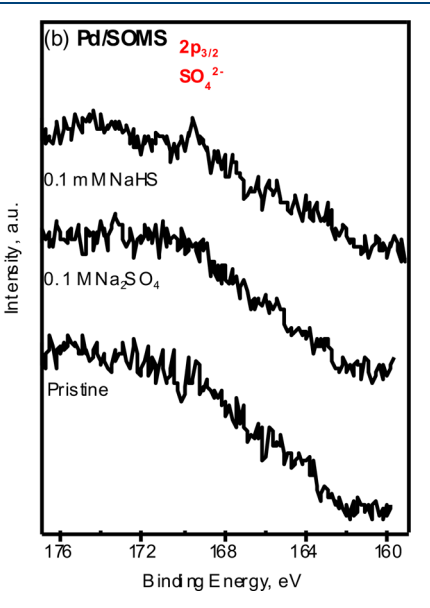


Figure 2. S 2p XPS spectra of pristine, Na<sub>2</sub>SO<sub>4</sub>-treated, and NaHS-treated (a) Pd/Al<sub>2</sub>O<sub>3</sub> and (b) Pd/SOMS.

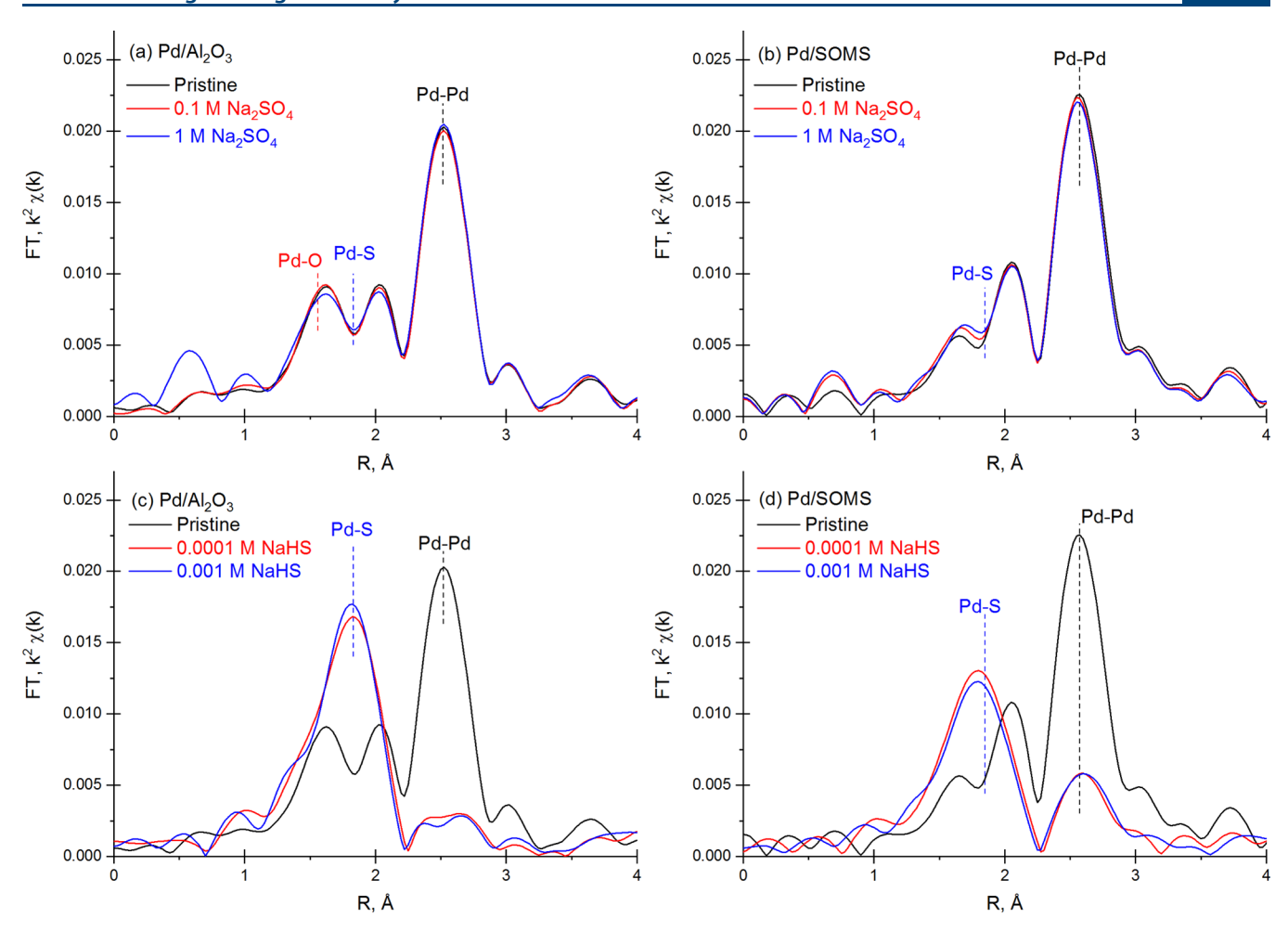


Figure 3.  $k^2$ -Weighted Fourier transform (FT) magnitudes of EXAFS spectra at the Pd K-edge. FT magnitudes of pristine and Na<sub>2</sub>SO<sub>4</sub>-treated (a) Pd/Al<sub>2</sub>O<sub>3</sub> and (b) Pd/SOMS, and pristine and NaHS-treated (c) Pd/Al<sub>2</sub>O<sub>3</sub> and (d) Pd/SOMS.

Table 2. Pd K-Edge EXAFS Fitting Results for Pristine, Na2SO4-Treated, and NaHS-Treated Pd/Al2O3 and Pd/SOMSa

	sample	XANES energy, keV	scatter	N	R, Å	$\Delta\sigma^2~(10^3)$	$E^0$ , eV
Pd/Al <sub>2</sub> O <sub>3</sub>	pristine	24.3517	Pd-Pd	6.5	2.74	2.0	-2.4
			Pd-O	1.4	2.05	2.0	1.6
	0.1 M Na <sub>2</sub> SO <sub>4</sub>	24.3521	Pd-Pd	6.4	2.74	2.0	-2.7
			Pd-O	1.5	2.05	2.0	1.3
	1 M Na <sub>2</sub> SO <sub>4</sub>	24.3521	Pd-Pd	6.6	2.74	2.0	-3.0
			Pd-O	1.4	2.05	2.0	1.2
	0.0001 M NaHS	24.3548	Pd-S	3.2	2.31	3.0	-0.4
	0.001 M NaHS	24.3544	Pd-S	3.2	2.31	3.0	-0.3
Pd/SOMS	pristine	24.3501	Pd-Pd	9.9	2.76	4.0	-1.1
	0.1 M Na <sub>2</sub> SO <sub>4</sub>	24.3502	Pd-Pd	9.7	2.76	4.0	-1.2
	1 M Na <sub>2</sub> SO <sub>4</sub>	24.3504	Pd-Pd	9.6	2.76	4.0	-1.4
	0.0001 M NaHS	24.3542	Pd-Pd	2.7	2.80	4.0	-5.1
			Pd-S	2.4	2.30	4.0	-1.0
	0.001 M NaHS	24. 3544	Pd-Pd	2.8	2.80	4.0	-5.8
			Pd-S	2.3	2.30	4.0	-0.7
$^{a}k^{2}$ : $\Delta k = 2.9-12$ .	$1 \text{ Å}^{-1}, \Delta R = 1-3 \text{ Å}; N$	$\pm 10\%$ , R $\pm 0.02$ .					

pristine catalyst does not have any sulfur-containing species on its surface. Upon treating  $Pd/Al_2O_3$  with solutions containing sulfur compounds, accumulation of sulfur species on its surface was observed. The deconvolution results of  $Pd/Al_2O_3$  treated with 0.1 M  $Na_2SO_4$  solution showed that sulfate species were partially converted to reduced sulfur species, including  $HS^-$  (161.8 eV) and  $SO_3^{\,2-}$  (165.3 eV).  $^{37-39}$  Conversion of sulfates

to reduced sulfur species is undesired, since reduced sulfur species are more deleterious than sulfates.  $^{6,12,13}$  The S 2p spectrum of Pd/Al<sub>2</sub>O<sub>3</sub> treated with 0.1 mM NaHS solution also showed that different forms of sulfur were present on its surface. The presence of  $\mathrm{SO_4}^{2-}$  and  $\mathrm{SO_3}^{2-}$  on the surface after HS $^-$  exposure indicates that oxidation of the sulfur species occurred.

The S 2p spectrum of pristine Pd/SOMS is shown in Figure 2b. No peaks were observed in the spectrum, indicating the absence of sulfur species on the surface. This is expected, since no sulfur-containing species were used in the synthesis and the pretreatment steps during the synthesis of SOMS and Pd/SOMS. The increase in the background signal is due to the plasmon loss feature of Si. 40,41 Similar to the pristine catalyst, the spectrum of Pd/SOMS treated with a 0.1 M Na<sub>2</sub>SO<sub>4</sub> solution did not exhibit any peaks due to the presence of sulfur species on its surface. This shows that sulfate species were not accumulated on the surface of Pd/SOMS. In the spectrum of Pd/SOMS treated with a 0.1 mM NaHS solution, there was no accumulation of sulfur on its surface, except that there was a peak having a low intensity at a binding energy of 169.3 eV, possibly indicating the presence of sulfate species.

3.1.3. Extended X-ray Absorption Fine Structure (EXAFS). The pristine and sulfur-treated samples of  $Pd/Al_2O_3$  and Pd/SOMS catalysts were examined by EXAFS spectroscopy at the Pd K-edge (24350 eV) to determine the changes in the atomic environment of Pd nanoparticles due to exposure to sulfur species. The pristine samples were treated with aqueous solutions of  $Na_2SO_4$  or NaHS at different concentrations. The  $k^2$ -weighted Fourier transform (FT) magnitudes and the coordination parameters of pristine and poisoned samples are given in Figure 3 and Table 2, respectively.

The EXAFS of pristine Pd/Al<sub>2</sub>O<sub>3</sub> consisted of Pd–Pd and Pd–O scatterings with coordination numbers of 6.5 and 1.4, respectively, indicating that Pd nanoparticles were slightly oxidized. The coordination number of 1.4 for Pd–O scattering corresponds to an average oxidation state of 0.7, since there are four Pd–O bonds in fully oxidized PdO. The true coordination number for Pd–Pd scattering was, however, approximately 10 since 65% of the Pd nanoparticles were metallic. A coordination number of 10 for Pd–Pd scattering indicated that the size of Pd nanoparticles on Al<sub>2</sub>O<sub>3</sub> was about 5 nm.<sup>42</sup>

The EXAFS of pristine Pd/SOMS only consisted of Pd–Pd scattering (Figure 3b), indicating that Pd NPs incorporated into SOMS are metallic. The coordination number of Pd/SOMS was obtained as 9.9, similar to the true coordination number of Pd/Al $_2$ O $_3$ . EXAFS fitting results also revealed that the bond distance for Pd–Pd was larger than that of Pd foil (2.75 Å). The increase in the bond distance could be attributed to formation of Pd–H species during the synthesis of Pd/SOMS.  $^{43,44}$ 

Parts a and b of Figure 3 show the FT magnitudes of EXAFS spectra for pristine and Na<sub>2</sub>SO<sub>4</sub>-exposed Pd/Al<sub>2</sub>O<sub>3</sub> and Pd/SOMS, respectively. As can be seen from the figures, the treatment with sulfate solutions at different concentrations did not alter the atomic environment of Pd significantly. This was also confirmed by the fitting results given in Table 2.

FT magnitudes for Pd/Al<sub>2</sub>O<sub>3</sub> poisoned with NaHS-containing solutions at different concentrations can be seen in Figure 3c. Two major changes were noted in the spectra of 0.1 mM NaHS-treated Pd/Al<sub>2</sub>O<sub>3</sub> in comparison to that of pristine sample, a large decrease in the magnitude of Pd–Pd scattering and the appearance of Pd–S scattering. The results indicate that the sulfur atoms were able to enter the atomic structure of Pd/Al<sub>2</sub>O<sub>3</sub> when the precursor for sulfur treatment was bisulfide. The Pd–Pd and Pd–S scattering magnitudes did not change noticeably as the concentration of the treatment solution was increased to 1 mM. Small amounts of metallic Pd could be present in these samples.

The  $k^2$ -weighted FT magnitudes of Pd/SOMS exposed to bisulfide-solutions are shown in Figure 3d. The FT magnitude of the pristine Pd/SOMS decreased significantly due to the poisoning treatment. However, the decrease of Pd–Pd scattering in the poisoned Pd/SOMS was less pronounced than that in the poisoned Pd/Al<sub>2</sub>O<sub>3</sub>. The fitting results, shown in Table 2, revealed that the coordination numbers for Pd–Pd and Pd–S in Pd/SOMS treated with 1 mM NaHS were 2.8 and 2.3, respectively. Under the same treatment conditions, the Pd–Pd scattering was retained in Pd/SOMS compared to Pd/Al<sub>2</sub>O<sub>3</sub>, indicating that Pd/SOMS is more resistant to bisulfides.

3.1.4. Exposure of Pd/SOMS to Sulfide Species in the Presence of Ethanol. The interactions of Pd nanoparticles with bisulfide molecules were investigated when Pd/SOMS matrix was swollen to different extents by changing the concentration of the swelling agent. Ethanol was chosen as the organic swelling agent.

Figure 4 shows the FT magnitude of the EXAFS spectra at the Pd K-edge of NaHS-treated Pd/SOMS samples in the

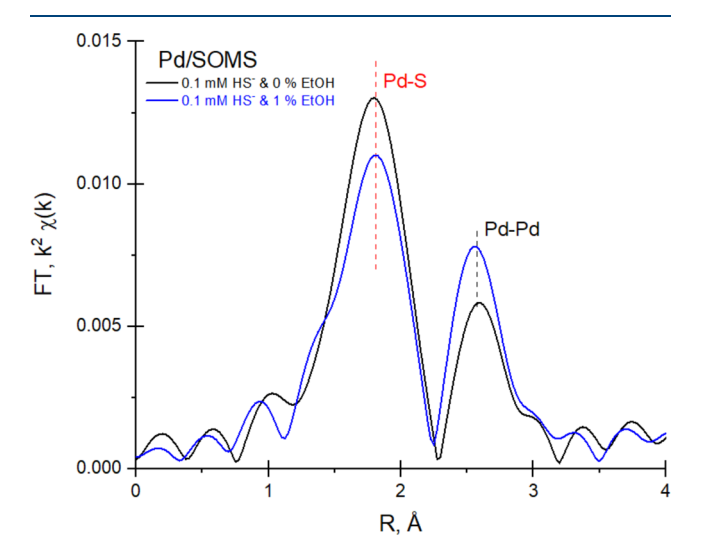


**Figure 4.**  $k^2$ -Weighted Fourier transform magnitude of EXAFS spectra at the Pd K-edge of NaHS-treated Pd/SOMS. The treatments were performed in the presence of 0% and 1% ethanol in 0.1 mM NaHS solution.

absence as well as in the presence of 1% ethanol in the sulfide solution. The concentration of bisulfide was kept constant at 0.1 mM. The EXAFS spectra of Pd/SOMS show that swelling of the SOMS matrix by ethanol did not facilitate the sulfidation of the Pd species. In fact, the presence of ethanol seems to alleviate the effect of the sulfide species.

As shown in Table 3, when aqueous NaHS solution containing 1% ethanol was used, the coordination number of Pd-S scattering decreased from 2.4 to 2.0 and that of Pd-Pd scattering was increased from 2.7 to 3.6, compared to the sample treated with NaHS in the absence of ethanol. This result was somewhat surprising, since the swelling of the SOMS matrix was expected to make the Pd sites more readily accessible to the poisoning effect of the sulfide species. The results, however, showed this not to be the case. Instead, the poisoning of Pd NPs appeared to be suppressed, possibly because of (i) the reducing ability of ethanol that slowed down the transformation of Pd-Pd to Pd-S during the treatment and (ii) changes in the pore solvent environment due to ethanol adsorption in the pores that may affect the solvation of

Table 3. Pd K-Edge EXAFS Fitting Results for NaHS-Treated<sup>a</sup> Pd/SOMS<sup>b</sup>

sample		XANES energy, keV	scatter	N	R, Å	$\Delta\sigma^2~(10^3)$	$E^0$ , eV		
	Pd/SOMS	0% ethanol	24.3542	Pd-Pd	2.7	2.80	4.0	-5.1	
				Pd-S	2.4	2.30	4.0	-1.0	
		1% ethanol	24.3546	Pd-Pd	3.6	2.78	4.0	-6.8	
				Pd-S	2.0	2.30	4.0	-0.3	

<sup>a</sup>The treatments were performed in the presence of 0.0% and 1% ethanol in 0.1 mM NaHS solution.  ${}^bk^2$ :  $\Delta k = 2.9-12.1 \text{ Å}^{-1}$ ,  $\Delta R = 1-3 \text{ Å}$ ;  $N \pm 10\%$ ,  $R \pm 0.02$ .

bisulfide anionic species. This result is significant in showing that the swelling of the SOMS matrix helps the accessibility of the Pd sites for the reaction, but does not change the partially protected nature of these sites from the deactivation effects of the poisons dissolved in water.

3.1.5. Temperature-programmed Reaction ( $TP_{rxn}$ ) with  $H_2$ . Temperature-programmed reaction experiments with  $H_2$  were performed to examine how easily the sulfur species would be removed from the surfaces of  $Pd/Al_2O_3$  and Pd/SOMS that were treated with solutions of 0.1 M  $SO_4^{2-}$ . The evolution of  $H_2S$  with respect to temperature was monitored by the m/z=34 signal of a mass spectrometer.

 $TP_{rxn}$  profiles of catalysts treated with NaSO<sub>4</sub> solution are shown in Figure 5. A broad  $H_2S$  evolution at 605  $^{\circ}C$  was

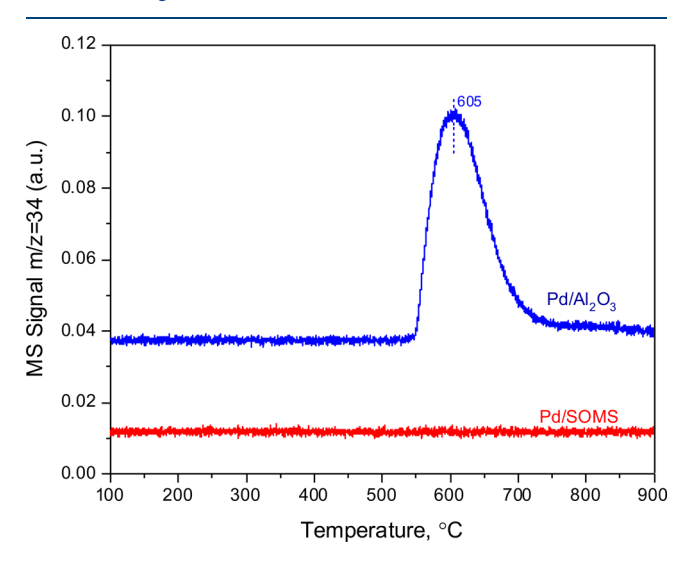


**Figure 5.** Temperature-programmed reaction with  $H_2$  over  $Pd/Al_2O_3$  and Pd/SOMS treated with 0.1 M  $Na_2SO_4$ . The m/z = 34 signal was followed to monitor the evolution of  $H_2S$ .

observed over  $Pd/Al_2O_3$ , indicating that  $H_2$  at high temperatures was able to remove the sulfur accumulated on the surface of alumina. The  $H_2S$  evolution over poisoned  $Pd/Al_2O_3$  stemmed from the sulfur adsorbed on alumina rather than Pd sites, since EXAFS results (section 3.2) clearly showed that the sulfate exposure did not result in Pd–S scattering in the atomic environment of Pd. It is, however, expected that prolonged exposure of  $Pd/Al_2O_3$  to the sulfate solution may cause Pd nanoparticles to be poisoned as well due to formation of reduced sulfur species and migration of these species to the Pd sites. When the  $TP_{\rm rxn}$  with  $H_2$  profile of Pd/SOMS poisoned by 0.1 M  $Na_2SO_4$  was examined, no evolution of  $H_2S$  was observed, indicating that the sulfate molecules did not adsorb on the surface of Pd/SOMS under the same experimental conditions.

3.1.6. Catalytic Activity Experiments. The aqueous-phase HDC of TCE activities Pd/Al<sub>2</sub>O<sub>3</sub> and Pd/SOMS samples were tested before and after exposure to aqueous sulfur species to examine the changes in the catalytic activity upon exposure to sulfates and bisulfides. Catalytic activity experiments were performed at 50 bar and 30 °C in batch mode. TCE conversions obtained over pristine catalysts are given in Figure 6. The pristine Pd/Al<sub>2</sub>O<sub>3</sub> outperformed the pristine Pd/SOMS throughout the reaction duration on the basis of equal catalyst amount. TCE conversions obtained over Pd/SOMS and Pd/ Al<sub>2</sub>O<sub>3</sub> at the end of 6 h were 62% and 89%, respectively. The differences in the catalytic activity of pristine catalysts were examined in more detail in our earlier work.<sup>23</sup> In the present investigation, the scope of the study was focused on the changes in the catalytic activity due to aqueous-phase treatments with sulfur-containing compounds.

The pristine Pd/Al<sub>2</sub>O<sub>3</sub> and Pd/SOMS catalysts were treated by 0.1 M Na<sub>2</sub>SO<sub>4</sub> for 1 h. Figure 6a shows conversions of TCE over pristine and Na<sub>2</sub>SO<sub>4</sub>-treated Pd/Al<sub>2</sub>O<sub>3</sub>. The catalytic activity of the pristine and Na2SO4-treated Pd/Al2O was observed to be the same throughout the reaction time. Similarly, the treatment with 0.1 M Na<sub>2</sub>SO<sub>4</sub> solution did not affect the catalytic activity of Pd/SOMS, as shown in Figure 6b. The activity experiments revealed that the catalytic performance of neither Pd/Al<sub>2</sub>O<sub>3</sub> nor Pd/SOMS was negatively affected by sulfate exposure. Our results are in agreement with previously performed studies that showed sulfates to have little to no effect on the catalytic activity of Pd/ Al<sub>2</sub>O<sub>3</sub> for HDC of chlorinated ethylenes.<sup>6,10,45</sup> This was attributed to the high oxidation state of sulfur and the shielding effect of the four oxygen atoms surrounding the sulfur atom.<sup>2</sup> It should, however, be mentioned that further exposure to sulfates, either by higher concentrations or by longer durations, may cause a decrease in the catalytic performance. XPS results presented in section 3.2 showed that sulfates were converted to reduced sulfur species such as  $SO_3^{2-}$  and HS<sup>-</sup>, which are known catalyst deactivators. <sup>1,6,8,12</sup>

The treatment with 0.1 mM bisulfide solution caused a dramatic decrease in the catalytic activity of Pd/Al<sub>2</sub>O<sub>3</sub>. Figure 6c shows the TCE conversions over pristine and bisulfide-treated Pd/Al<sub>2</sub>O<sub>3</sub>. Upon the bisulfide treatment, TCE conversion achieved at the end of the reaction duration decreased from 89% to 35%. The catalytic activity decrease observed over Pd/SOMS due to bisulfide-poisoning, however, was not as pronounced as seen in Figure 6d. Although TCE conversions observed over pristine and NaHS-treated Pd/SOMS were similar in the first 90 min of the reaction, TCE conversion over bisulfide-treated Pd/SOMS showed a plateau, possibly due to inhibition of the Pd sites by the reaction product HCl. The inhibition due to HCl is expected to be more prominent on the sulfur-free metallic Pd sites in the treated sample compared to the Pd sites available in the

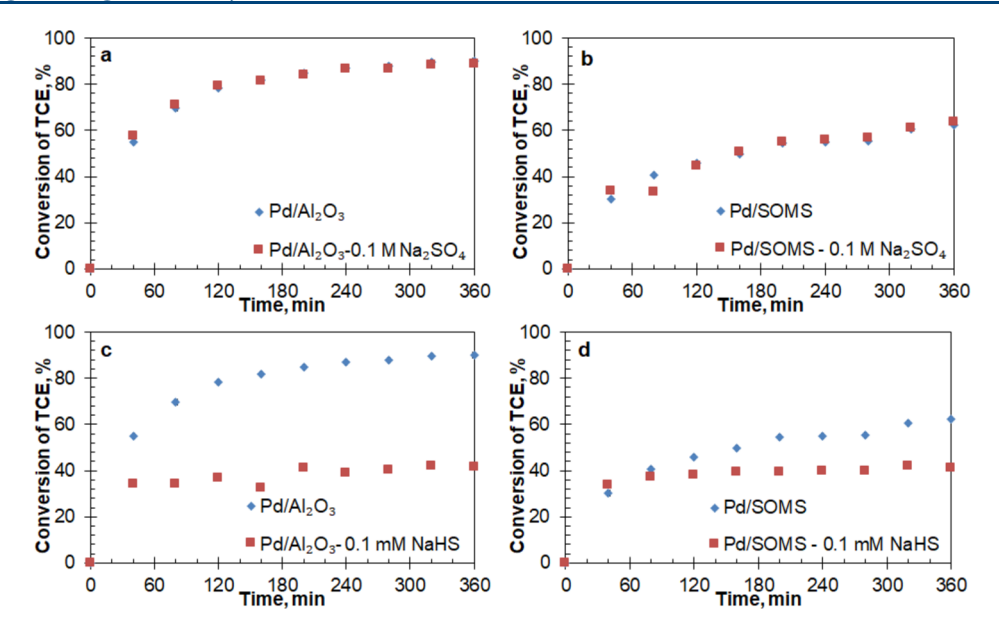


Figure 6. Comparison of catalytic activities over pristine and poisoned  $Pd/Al_2O_3$  and Pd/SOMS. Effect of 0.1 M  $Na_2SO_4$  treatment over (a)  $Pd/Al_2O_3$  and (b) Pd/SOMS and effect of 0.1 mM NaHS treatment over (c)  $Pd/Al_2O_3$  and (d) Pd/SOMS. Reaction conditions: 50 bar, 30 °C, 0.025 (mg cat.)/(mL solution),  $[TCE]_0 = 250$  ppm.

pristine Pd/SOMS, since the extent of the inhibition depends on the concentration of metallic Pd sites

**3.2.** Effect of Exposure to Sulfur Species in the Gas Phase. 3.2.1. EXAFS Analysis. Due to its relevance to gasphase HDC of TCE, sulfur treatment experiments were also performed in the gas phase by using concentrated  $\rm H_2S$  as the source of sulfur. As described in the experimental section, sulfur exposure experiments were performed over  $\rm Pd/Al_2O_3$  and  $\rm Pd/SOMS$  at 250 °C by using a gas stream of 800 ppm of  $\rm H_2S$ , 25%  $\rm H_2$ , and balance He. The changes in the Kronig structure of Pd due to the sulfur treatment were examined by EXAFS spectroscopy at the Pd K-edge. Figure 7 shows the  $k^2$ -weighted Fourier transform magnitude of EXAFS spectra of pristine and  $\rm H_2S$ -treated  $\rm Pd/Al_2O_3$  and  $\rm Pd/SOMS$ . The EXAFS coordination parameters are tabulated in Table 4.

The sulfur treatment converted all of the Pd scatterings (Pd–Pd and Pd–O) present in the pristine Pd/Al<sub>2</sub>O<sub>3</sub> into a single Pd–S scattering. The H<sub>2</sub>S-treated Pd/Al<sub>2</sub>O<sub>3</sub> lost almost all of Pd–Pd scattering. In the case of Pd/SOMS, however, most of the magnitude of the Pd–Pd scattering was intact. Some of the Pd nanoparticles were bound to sulfur, as evidenced by the appearance of a Pd–S scattering in Figure 7. The fitting results revealed that the coordination numbers of Pd–Pd and Pd–S scattering in H<sub>2</sub>S-treated Pd/SOMS were 8.2 and 1.4, respectively. The interatomic bond distance of Pd NPs shifted to 2.82 Å. The increase of the bond distance was attributed to formation of PdH<sub>x</sub> species that possibly formed during the sulfur treatment. 43,44 No information was obtained about the PdH<sub>x</sub> formation over Pd/Al<sub>2</sub>O<sub>3</sub>, since the sulfur treatment converted all of the metallic Pd to sulfur-bound Pd.

The results are significant to show the sulfur-resistant characteristics of Pd/SOMS in the gas phase. The high sulfur resistance can be attributed to the polarity of the  $H_2S$  molecule, which may be considered as too polar to enter the hydrophobic matrix of Pd/SOMS.

3.2.2. Temperature-programmed Reaction ( $TP_{rxn}$ ) with  $H_2$ . Pd/Al<sub>2</sub>O<sub>3</sub> and Pd/SOMS catalysts exposed to H<sub>2</sub>S in the gas phase were subjected to  $TP_{rxn}$  with H<sub>2</sub>. As shown by the m/z =

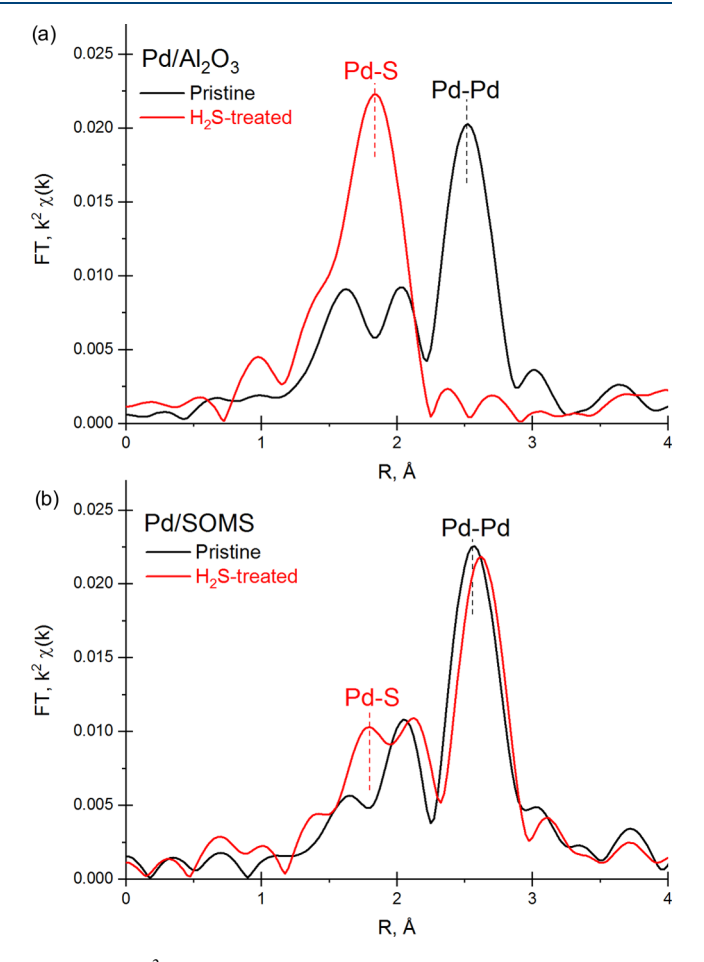


Figure 7.  $k^2$ -Weighted Fourier transform magnitude of EXAFS spectra at the Pd K-edge of pristine and gas-phase H<sub>2</sub>S-treated (a) Pd/Al<sub>2</sub>O<sub>3</sub> and (b) Pd/SOMS.

34 signal in Figure 8,  $Pd/Al_2O_3$  showed a strong  $H_2S$  evolution around 365 °C, followed by a smaller peak at around 725 °C, suggesting that there were two types of sulfur species on the

Table 4. Pd K-Edge EXAFS Fitting Results for Pristine and Gas-Phase H<sub>2</sub>S-Treated Pd/Al<sub>2</sub>O<sub>3</sub> and Pd/SOMS<sup>a</sup>

sample		XANES energy, keV	scatter	N	R, Å	$\Delta\sigma^2~(10^3)$	$E^0$ , eV
Pd/Al <sub>2</sub> O <sub>3</sub>	pristine	24.3517	Pd-Pd	6.5	2.74	2.0	-2.4
			Pd-O	1.4	2.05	2.0	1.6
	H <sub>2</sub> S-treated	24.3550	Pd-S	3.7	2.31	1.8	-0.5
Pd/SOMS	pristine	24.3501	Pd-Pd	9.9	2.76	4.0	-1.1
	H <sub>2</sub> S-treated	24.3550	Pd-Pd	8.2	2.82	2.5	-2.0
			Pd-S	1.4	2.31	4.0	3.4
${}^{a}k^{2}$ . $\Delta k = 2.9 - 12.1 \text{ Å}^{-1}$ , $\Delta R = 1 - 3 \text{ Å}$ : $N + 10\%$ , $R + 0.02$ .							

Pd/Al<sub>2</sub>O<sub>3</sub> Pd/SOMS 0.03 0.03 MS signal m/z=34, (a.u.) MS signal m/z=34, (a.u.) 0.02 0.02 0.01 0.01 400 600 800 200 200 400 600 800 Temperature (°C) Temperature (°C)

Figure 8. Temperature-programmed reaction with  $H_2$  over  $Pd/Al_2O_3$  and Pd/SOMS treated with  $H_2S$  in the gas phase. The m/z = 34 signal was followed to monitor the evolution of  $H_2S$ .

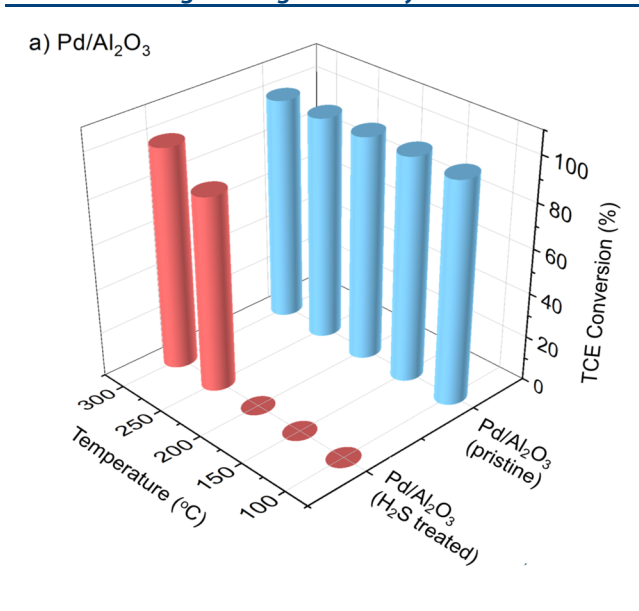
 $Pd/Al_2O_3$ , one weakly bound and one much more strongly bound. In case of Pd/SOMS, however, there is only the low-temperature  $H_2S$  evolution peak, but with a much lower intensity. The high-temperature peak seen over  $Pd/Al_2O_3$  is not present in the case of Pd/SOMS, showing that the extent of interaction of the Pd sites with the sulfur species is much higher over  $Pd/Al_2O_3$ . This is consistent with the EXAFS results (Figure 7), wherein interaction with  $H_2S$  led to the formation of very few Pd-S bonds in Pd/SOMS, whereas  $Pd/Al_2O_3$  showed almost complete sulfidation.

3.2.3. Catalytic Activity Experiments. Figure 9 shows the catalytic activity of pristine and H<sub>2</sub>S-treated Pd/SOMS and Pd/Al<sub>2</sub>O<sub>3</sub> catalysts in the gas-phase HDC of TCE reaction at 100-300 °C. As can be seen, while the activities of pristine and H<sub>2</sub>S-treated Pd/SOMS were very close to each other even at low temperatures, the deactivation effect of H<sub>2</sub>S treatment was very significant over Pd/Al<sub>2</sub>O<sub>3</sub>, which did not show any TCE conversion until the reaction temperature reached 250 °C. This is consistent with EXAFS and TP<sub>rxn</sub> results, where sulfur was found to be bound to the Pd sites over Pd/Al<sub>2</sub>O<sub>3</sub> to a much larger extent than over Pd/SOMS. Although the evolution of the H<sub>2</sub>S signal from the Pd/Al<sub>2</sub>O<sub>3</sub> surface does not start until a temperature higher than 250 °C is reached in the H<sub>2</sub>-TP<sub>rxn</sub> experiment, this is expected because activity data are collected under isothermal conditions at the steady state, whereas in the TP<sub>rxn</sub> experiment the temperature is ramped using a linear temperature program.

# 4. CONCLUSIONS

The sulfur-resistance characteristics of Pd/SOMS and Pd/ Al<sub>2</sub>O<sub>3</sub> were investigated both in the liquid phase and in the gas phase. The textural properties of Pd/Al<sub>2</sub>O<sub>3</sub> were seen to change after aqueous-phase exposure to sulfate and bisulfide species; however, this is found to be due to exposure to water and not necessarily to sulfur compounds. A significant amount of sulfur-accumulation was observed on the surface of alumina when the treatment was performed with sulfates or bisulfides. Unlike sulfate poisoning, bisulfide poisoning lowered the catalytic activity of Pd/Al<sub>2</sub>O<sub>3</sub> and resulted in chemisorption of sulfur on the active Pd sites. Pd/SOMS, however, exhibited better resistance to sulfur deactivation than Pd/Al<sub>2</sub>O<sub>3</sub>. The textural properties remained unaffected by the sulfur treatments. Treatment of Pd/SOMS with sulfates did not result in sulfur accumulation on the surface and did not lower the catalytic activity. Although exposure to bisulfides led to partial sulfidation of Pd NPs on SOMS, the extent of deactivation was much less prominent compared to that of Pd/Al<sub>2</sub>O<sub>3</sub>.

Furthermore, Pd/SOMS exhibited remarkable resistance to sulfur in the gas phase, while all of the metallic Pd nanoparticles on H<sub>2</sub>S-treated Pd/Al<sub>2</sub>O<sub>3</sub> were found to be bound to sulfur. Gas-phase TCE hydrodechlorination experiments showed no deactivation effect over Pd/SOMS, while the deactivation was very pronounced over Pd/Al<sub>2</sub>O<sub>3</sub>. The removal of sulfur from H<sub>2</sub>S-treated Pd/SOMS was shown to be more facile than that over Pd/Al<sub>2</sub>O<sub>3</sub>, suggesting easier regeneration of the catalysts.



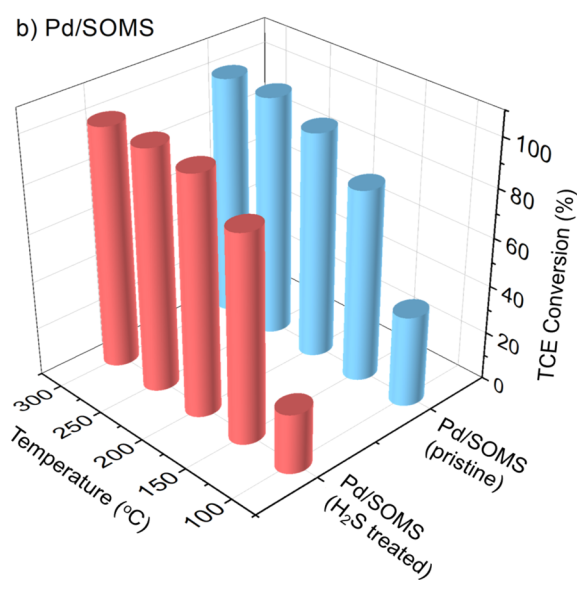


**Figure 9.** Comparison of catalytic activities over pristine and  $H_2S$ -treated  $Pd/Al_2O_3$  and Pd/SOMS. Effect of gas-phase  $H_2S$  treatment over (a)  $Pd/Al_2O_3$  and (b) Pd/SOMS.

In conclusion, the unique characteristics of the SOMS scaffold, such as hydrophobicity and high affinity for organics, allow the formulation of a Pd-based water treatment catalyst with better resistance to deactivation with sulfur species than its commercially used counterpart Pd/Al<sub>2</sub>O<sub>3</sub>. The sulfur resistance could be further improved by designing bimetallic catalysts in which Pd sites are stabilized in an electron-deficient state.

# ASSOCIATED CONTENT

#### S Supporting Information

The Supporting Information is available free of charge on the ACS Publications website at DOI: 10.1021/acs.iecr.8b05979.

XPS deconvolution results obtained for pristine and deconvoluted  $Pd/Al_2O_3$  (PDF)

### AUTHOR INFORMATION

## **Corresponding Author**

\*E-mail: ozkan.1@osu.edu. Tel: (614)-292-6623.

# ORCID ®

Umit S. Ozkan: 0000-0001-5571-2257

#### Notes

The authors declare no competing financial interest.

#### ACKNOWLEDGMENTS

The financial support for this work was provided by the National Science Foundation through Grant CBET-1436729 and the Ohio Coal Research Consortium. The authors wish to thank Dr. Lisa Hommel for her assistance with XPS data acquisition. J.T.M. was supported as part of the National Science Foundation Energy Research Center for Innovative and Strategic Transformation of Alkane Resources (CISTAR) under the Cooperative Agreement No. EEC-1647722. This study made use of the Materials Research Collaborative Access Team's (MRCAT) sector 10-ID-B. MRCAT operations are supported by the Department of Energy and the MRCAT member institutions. This research used resources of the Advanced Photon Source, a U.S. Department of Energy (DOE) Office of Science User Facility operated for the DOE Office of Science by Argonne National Laboratory under Contract No. DE-AC02-06CH11357.

#### REFERENCES

- (1) Munakata, N.; Reinhard, M. Palladium-catalyzed aqueous hydrodehalogenation in column reactors: Modeling of deactivation kinetics with sulfide and comparison of regenerants. *Appl. Catal., B* **2007**, 75 (1-2), 1-10.
- (2) Barbier, J.; Lamy-Pitara, E.; Marecot, P.; Boitiaux, J. P.; Cosyns, J.; Verna, F. Role of Sulfur in Catalytic Hydrogenation Reactions. In *Advances in Catalysis*; Eley, D. D., Pines, H., Weisz, P. B., Eds.; Academic Press, 1990; Vol. 37, pp 279–318.
- (3) Bartholomew, C. H. Mechanisms of catalyst deactivation. *Appl. Catal., A* **2001**, 212 (1–2), 17–60.
- (4) Maxted, E. B. The Poisoning of Metallic Catalysts. In *Advances in Catalysis*; Frankenburg, W. G., Komarewsky, V. I., Rideal, E. K., Emmett, P. H., Taylor, H. S., Eds.; Academic Press, 1951; Vol. 3, pp 129–178.
- (5) Lowry, G. V.; Reinhard, M. Hydrodehalogenation of 1-to 3-carbon halogenated organic compounds in water using a palladium catalyst and hydrogen gas. *Environ. Sci. Technol.* **1999**, 33 (11), 1905—1910.
- (6) Lowry, G. V.; Reinhard, M. Pd-catalyzed TCE dechlorination in groundwater: Solute effects, biological control, and oxidative catalyst regeneration. *Environ. Sci. Technol.* **2000**, 34 (15), 3217–3223.
- (7) López, E.; Ordóñez, S.; Díez, F. V. Inhibition effects of organosulphur compounds on the hydrodechlorination of tetrachloroethylene over Pd/Al2O3 catalysts. *Catal. Today* **2003**, 84 (3–4), 121–127.
- (8) Angeles-Wedler, D.; Mackenzie, K.; Kopinke, F.-D. Sulphide-induced deactivation of Pd/Al2O3 as hydrodechlorination catalyst and its oxidative regeneration with permanganate. *Appl. Catal., B* **2009**, *90* (3–4), 613–617.
- (9) Kopinke, F.-D.; Angeles-Wedler, D.; Fritsch, D.; Mackenzie, K. Pd-catalyzed hydrodechlorination of chlorinated aromatics in contaminated waters—Effects of surfactants, organic matter and catalyst protection by silicone coating. *Appl. Catal., B* **2010**, *96* (3), 323–328
- (10) Schreier, C. G.; Reinhard, M. Catalytic hydrodehalogenation of chlorinated ethylenes using palladium and hydrogen for the treatment of contaminated water. *Chemosphere* **1995**, *31* (6), 3475–3487.

- (11) Sulfate in Drinking-Water, Background Document for Development of WHO Guidelines for Drinking-Water Quality; World Health Organization, 2004.
- (12) Angeles-Wedler, D.; Mackenzie, K.; Kopinke, F.-D. Permanganate Oxidation of Sulfur Compounds to Prevent Poisoning of Pd Catalysts in Water Treatment Processes. *Environ. Sci. Technol.* **2008**, 42 (15), 5734–5739.
- (13) Davie, M. G.; Cheng, H.; Hopkins, G. D.; LeBron, C. A.; Reinhard, M. Implementing heterogeneous catalytic dechlorination technology for remediating TCE-contaminated groundwater. *Environ. Sci. Technol.* **2008**, *42* (23), 8908–8915.
- (14) Nutt, M. O.; Hughes, J. B.; Wong, M. S. Designing Pd-on-Au Bimetallic Nanoparticle Catalysts for Trichloroethene Hydrodechlorination. *Environ. Sci. Technol.* **2005**, 39 (5), 1346–1353.
- (15) Nutt, M. O.; Heck, K. N.; Alvarez, P.; Wong, M. S. Improved Pd-on-Au bimetallic nanoparticle catalysts for aqueous-phase trichloroethene hydrodechlorination. *Appl. Catal., B* **2006**, *69* (1–2), 115–125.
- (16) Heck, K. N.; Nutt, M. O.; Alvarez, P.; Wong, M. S. Deactivation resistance of Pd/Au nanoparticle catalysts for waterphase hydrodechlorination. *J. Catal.* **2009**, 267 (2), 97–104.
- (17) Schüth, C.; Disser, S.; Schüth, F.; Reinhard, M. Tailoring catalysts for hydrodechlorinating chlorinated hydrocarbon contaminants in groundwater. *Appl. Catal., B* **2000**, 28 (3), 147–152.
- (18) Schüth, C.; Kummer, N.-A.; Weidenthaler, C.; Schad, H. Field application of a tailored catalyst for hydrodechlorinating chlorinated hydrocarbon contaminants in groundwater. *Appl. Catal., B* **2004**, *52* (3), 197–203.
- (19) Fritsch, D.; Kuhr, K.; Mackenzie, K.; Kopinke, F.-D. Hydrodechlorination of chloroorganic compounds in ground water by palladium catalysts: Part 1. Development of polymer-based catalysts and membrane reactor tests. *Catal. Today* **2003**, 82 (1), 105–118.
- (20) Navon, R.; Eldad, S.; Mackenzie, K.; Kopinke, F.-D. Protection of palladium catalysts for hydrodechlorination of chlorinated organic compounds in wastewaters. *Appl. Catal., B* **2012**, *119*–120, 241–247.
- (21) Celik, G.; Ailawar, S. A.; Sohn, H.; Tang, Y.; Tao, F. F.; Miller, J. T.; Edmiston, P. L.; Ozkan, U. S. Swellable Organically Modified Silica (SOMS) as a Catalyst Scaffold for Catalytic Treatment of Water Contaminated with Trichloroethylene. *ACS Catal.* **2018**, *8*, 6796–6809
- (22) Celik, G.; Ailawar, S. A.; Gunduz, S.; Edmiston, P. L.; Ozkan, U. S. Formation of carbonaceous deposits on Pd-based hydrodechlorination catalysts: Vibrational spectroscopy investigations over Pd/Al2O3 and Pd/SOMS. *Catal. Today* **2019**, 323, 129.
- (23) Celik, G.; Ailawar, S. A.; Gunduz, S.; Miller, J. T.; Edmiston, P. L.; Ozkan, U. S. Aqueous-phase hydrodechlorination of trichloroethylene over Pd-based swellable organically-modified silica (SOMS): Catalyst deactivation due to chloride anions. *Appl. Catal., B* **2018**, 239, 654–664.
- (24) Sohn, H.; Celik, G.; Gunduz, S.; Dean, S. L.; Painting, E.; Edmiston, P. L.; Ozkan, U. S. Hydrodechlorination of trichloroethylene over Pd supported on swellable organically-modified silica (SOMS). *Appl. Catal., B* **2017**, *203*, 641–653.
- (25) Sohn, H.; Celik, G.; Gunduz, S.; Majumdar, S. S.; Dean, S. L.; Edmiston, P. L.; Ozkan, U. S. Effect of high-temperature on the swellable organically-modified silica (SOMS) and its application to gas-phase hydrodechlorination of trichloroethylene. *Appl. Catal., B* **2017**, 209, 80–90.
- (26) Burkett, C. M.; Edmiston, P. L. Highly swellable sol—gels prepared by chemical modification of silanol groups prior to drying. *J. Non-Cryst. Solids* **2005**, 351 (40–42), 3174–3178.
- (27) Burkett, C. M.; Underwood, L. A.; Volzer, R. S.; Baughman, J. A.; Edmiston, P. L. Organic—Inorganic Hybrid Materials that Rapidly Swell in Non-Polar Liquids: Nanoscale Morphology and Swelling Mechanism. *Chem. Mater.* **2008**, *20* (4), 1312–1321.
- (28) Edmiston, P. L.; Underwood, L. A. Absorption of dissolved organic species from water using organically modified silica that swells. Sep. Purif. Technol. 2009, 66 (3), 532–540.

- (29) Edmiston, P. L.; Gilbert, A. R.; Harvey, Z.; Mellor, N. Adsorption of short chain carboxylic acids from aqueous solution by swellable organically modified silica materials. *Adsorption* **2018**, 24 (1), 53–63.
- (30) Ressler, T. WinXAS: A new software package not only for the analysis of energy-dispersive XAS data. J. Phys. IV 1997, 7, C2-269.
- (31) Pazmino, J. H.; Bai, C. S.; Miller, J. T.; Ribeiro, F. H.; Delgass, W. N. Effects of Support on Sulfur Tolerance and Regeneration of Pt Catalysts Measured by Ethylene Hydrogenation and EXAFS. *Catal. Lett.* **2013**, *143* (11), 1098–1107.
- (32) Sing, K. S. W. Reporting physisorption data for gas/solid systems with special reference to the determination of surface area and porosity (Recommendations 1984). *Pure Appl. Chem.* **1985**, *57* (4), 603–619.
- (33) Tsyurupa, M. P.; Davankov, V. A. Porous structure of hypercrosslinked polystyrene: State-of-the-art mini-review. *React. Funct. Polym.* **2006**, *66* (7), 768–779.
- (34) Groen, J. C.; Peffer, L. A. A.; Pérez-Ramírez, J. Pore size determination in modified micro- and mesoporous materials. Pitfalls and limitations in gas adsorption data analysis. *Microporous Mesoporous Mater.* **2003**, *60* (1), 1–17.
- (35) Peri, J. B.; Hannan, R. B. Surface Hydroxyl Groups on γ-Alumina1. *J. Phys. Chem.* **1960**, *64* (10), 1526–1530.
- (36) Deo, A. V.; Dalla Lana, I. G. Infrared study of the adsorption and mechanism of surface reactions of 1-propanol on.gamma.-alumina and.gamma.-alumina doped with sodium hydroxide and chromium oxide. *J. Phys. Chem.* **1969**, 73 (3), 716–723.
- (37) Moulder, J. F.; Chastain, J. Handbook of X-ray Photoelectron Spectroscopy: A Reference Book of Standard Spectra for Identification and Interpretation of XPS Data; Perkin-Elmer Corp., Physical Electronics Division, 1992.
- (38) Lindberg, B. J.; Hamrin, K.; Johansson, G.; Gelius, U.; Fahlman, A.; Nordling, C.; Siegbahn, K. Molecular Spectroscopy by Means of ESCA II. Sulfur compounds. Correlation of electron binding energy with structure. *Phys. Scr.* **1970**, *1* (5–6), 286.
- (39) Paál, Z.; Matusek, K.; Muhler, M. Sulfur adsorbed on Pt catalyst: its chemical state and effect on catalytic properties as studied by electron spectroscopy and n-hexane test reactions. *Appl. Catal., A* **1997**, *149* (1), 113–132.
- (40) Hassan, F. M.; Batmaz, R.; Li, J.; Wang, X.; Xiao, X.; Yu, A.; Chen, Z. Evidence of covalent synergy in silicon—sulfur—graphene yielding highly efficient and long-life lithium-ion batteries. *Nat. Commun.* **2015**, *6*, 8597.
- (41) Bozso, F.; Yates, J. T., Jr.; Choyke, W. J.; Muehlhoff, L. Studies of SiC formation on Si (100) by chemical vapor deposition. *J. Appl. Phys.* **1985**, *57* (8), 2771–2778.
- (42) Miller, J. T.; Kropf, A. J.; Zha, Y.; Regalbuto, J. R.; Delannoy, L.; Louis, C.; Bus, E.; van Bokhoven, J. A. The effect of gold particle size on Au-Au bond length and reactivity toward oxygen in supported catalysts. *J. Catal.* **2006**, 240 (2), 222–234.
- (43) Tew, M. W.; Miller, J. T.; van Bokhoven, J. A. Particle Size Effect of Hydride Formation and Surface Hydrogen Adsorption of Nanosized Palladium Catalysts: L-3 Edge vs K Edge X-ray Absorption Spectroscopy. *J. Phys. Chem. C* **2009**, *113* (34), 15140–15147.
- (44) McCaulley, J. A. In-situ x-ray absorption spectroscopy studies of hydride and carbide formation in supported palladium catalysts. *J. Phys. Chem.* **1993**, 97 (40), 10372–10379.
- (45) McNab, W. W.; Ruiz, R.; Reinhard, M. In-situ destruction of chlorinated hydrocarbons in groundwater using catalytic reductive dehalogenation in a reactive well: Testing and operational experiences. *Environ. Sci. Technol.* **2000**, 34 (1), 149–153.